Proteome Analysis of Testicular Tissue in Varicocele Rats Using iTRAQ Labeling Technology

lu xian feng
Pediatrics department, shanxi provincial people's hospital affiliated to shanxi medical university,shanxi,china

zhao wei
biochemistry and molecular biology, basic medical college,shanxi medical university,shanxi,china.

liu jian rong
reproductive medical department,shanxi provincial people's hospital affiliated to shanxi medical university,shanxi,china.

wang dan feng
biochemistry and molecular biology,basic medical college,shanxi medical university,shanxi,china

yuan cai xia
reproductive medical department,shanxi provincial people's hospital affiliated to shanxi medical university,shanxi,china

wang yi min
central laboratory, shaxi provincial people's hospital affiliated to shanxi medical university,shanxi,china

zhang fang
central laboratory,Shanxi Provincial People's Hospital affiliated to shanxi medicaluniversity,shanxi,china

Qin Qin (qinqin@sxmu.edu.cn)
department of reproductive medical department, shanxi provincial people's hospital, affiliated of shanxi medical university.

Research

Keywords: Varicocele, Proteomics, iTRAQ analysis, CIB1, ATP7A

Posted Date: February 12th, 2020

DOI: https://doi.org/10.21203/rs.2.23293/v1

Abstract

Purpose

Varicocele (VC) is considered as the main cause of male infertility, clear and definite molecular markers of varicocele disease are helpful for early prevention and timely treatment. This study was in order to examine the effect of varicocele on protein expression in testicular tissue.

Methods

The testicular tissue samples of normal rats and varicocele rats were used for proteomic analysis and functional bioinformatics analysis. The proteins with a fold change of > 1.2 or < 1.2, and with a P-value < 0.05 were used to identify up- and downregulation proteins between the varicocele and control rats, and two target proteins were selected and verified with western blot.

Results

It was found that seminiferous epithelium was disordered and spermatogenic cells were injured seriously in varicocele group. A total of 65 differentially expressed proteins were identified compared with normal group by liquid chromatography tandem mass spectrometry (LC-MS/MS) and isobaric tags for relative and absolute quantitation (iTRAQ) analysis, including 31 up-regulated proteins and 34 down-regulated proteins, respectively. Functions of those proteins were mainly related to the following processes: signal transduction, protein cycle, transmembrane transport, protein transport, vesicular mediated transport, cell division, and membrane tissue. Two down regulated proteins of ATPase and Cu^{2+}-transporting alpha (ATP7A) and Calcium and integrin-binding protein 1 (CIB1) in varicocele rats were selected and confirmed.

Conclusion

Protein spectrum of testicular tissue in varicocele rats was different from that in normal rats. Low expressions of ATP7A and CIB1 may be affect testicular spermatogenic function and can be used as a potential biomarker for testicular tissue to maintain normal spermatogenic function.

Introduction

Varicocele (VC) is a kind of vascular disease, and characterized by varying degrees of dilation and tortuosity of the spermatic veins [1]. VC can lead to male infertility, the incidence of VC in the common male population was 4.4-22.6 %, of which the incidence of primary infertility was 35-40 %, while the incidence of secondary infertility was as high as 80% [2, 3]. Now, the main causes of varicocele are included testicular hypoxia, oxidative stress, elevated local temperature, apoptosis of spermatogenic cells, nitric oxide, endocrine system dysfunction [4, 5]. However, the exact pathophysiological mechanism of male infertility caused by varicocele is still unclear.

At present, the study of varicocele infertility has been deeply studied in the molecular mechanism. Our previous research found the abberant expression of stem cell factor (SCF) and c-KIT in the testes of VC rats and speculated that VC induced spermatogenesis disorder was related to the abnormal expression of SCF/C-KIT system [6]. We also found the correlation between the apoptosis of spermatogenic cells and overexpression of hypoxia-inducible factor-1α (HIF-1α) in VC rats. By decreasing the expression of HIF-1α, the apoptosis of spermatogenic cells was reduced, which is beneficial to the recovery of testicular function and the improvement of fertility [7]. Liang et al. observed that increased expression level of reactive oxygen species (ROS) and p53 in VC rats and thought that the increased expression of p53 gene in testicular tissue was caused by the activation of ROS, and the abnormal increase of p53 may inhibit angiogenesis by generating anti-angiogenic factors, which lead to an increase in cell death [8, 9]. Hou et al. hold that the deletion of Magea gene could activate the expression of p53 gene, which could increase the apoptosis of spermatogenic cells and lead to male infertility [10].

In order to further explore the molecules involved in VC infertility, this is the first time to use iTRAQ combined with LC-MS/MS technique to screen the differential proteins in testis between VC rats and normal rats. According to the results of proteome analysis, the molecules that affected the spermatogenesis were selected for verification, which laid a foundation for further exploration of its role in VC infertility.

Materials And Methods

Animals

Twelve male Sprague Dawley rats weighing 200-250g were randomly divided into two groups, named normal group (n=6) and the varicocele group (n=6), respectively. All rats were fed the same diet and raised in a constant environment with a 12-hour light/dark cycle.

Establishment of the VC model

The rats of VC model were referenced from Turner [11]. All experimental procedures were performed in a sterile environment. The rats were anesthetized with an intraperitoneal injection of pentobarbital sodium 40 mg/kg. A midline laparotomy incision was made from xyphoid to pubis to visualize the left renal vein, inferior vena cava, left spermatic vein, left suprarenal vein, and left kidney. Following a careful blunt dissection, a clamp was passed behind the left renal vein just distal to the spermatic vein insertion, a loose ligature of 4-zero silk was placed around the left renal vein at the site, and a rigid hydrophilic 0.8-mm-diameter guide wire was placed on the left renal vein. The ligature was tied around the vein over the top of the guide wire, and the wire was withdrawn, allowing vein diameter to be reduced to approximately half of normal. After the injection of penicillin into the abdominal cavity, the midline incision was closed in two layers using 4/0 silk sutures. Successful modeling criteria: the diameter of the spermatic vein was more than 1mm and there was no difference in size between the left and right kidneys [11, 12]. And the control group did not do any treatment. All animals were sacrificed after 8 weeks, and the testicular tissue

was extracted immediately after the rats were euthanized by intravenous injection of pentobarbital sodium.

Hematoxylin and eosin staining

HE staining was conducted according to routine protocols [7]. After fixation in 4% paraformaldehyde and dehydrated sequentially with ethanol, the left testicle tissue was embedded in paraffin and sectioned at 5 um thickness. After routine dewaxing and hydration, sections were stained with hematoxylin for 5 min and eosin for 2 min. The morphology of seminiferous tubules was observed under an optical microscope.

Protein extraction, quantification, and digestion

These processes were conducted according to routine protocols [13]. Three rats were randomly selected from each group for the experiment. Samples were dissolved in lysis buffer (consisting of 7M urea, 1.4M thiourea, 0.1% 3-[(3-cholamidopropyl)-dimethylammonio]-1-propane sulfonate (CHAPS)) and fully mixed, and then centrifuged at 14,000 g for 30 min at 4°C. The supernatant was collected and the protein concentration was determined according to the Bradford method. 100μg of each sample was added into 4μl of reducing reagent (60℃, 1h), then 2μl of Cysteine-Blocking reagent was mixed into it (room temperature (RT), 10min). The reductive alkylation protein solution was added into a 10K ultrafiltration tube (12,000r, 20min), the solution in the bottom was discarded, and then 100μl of dissolution buffer of the iTRAQ kit was added into it (12,000r, 20min). A new collection tube was used to add trypsin and to react with the acquired solution (37℃, overnight). Next day, the peptide solution digested by enzyme hydrolysis was collected at the bottom of the tube (12,000r, 20min). 50μl of dissolution buffer 5 (12,000r, 20min) was combined with the above products, then 100μl of sample was obtained which is after digestion at the bottom of the collection tube.

Protein labeling with iTRAQ

50μl of sample (100μg of hydrolyzed product) was added into the iTRAQ reagent which contained 150μl of isopropanol, and was centrifuged at the bottom of the tube after vortex oscillation (RT, 2h). 100μl of water was added to terminate the reaction. Labeling was performed according to the manufacturer's instructions (Applied Biosystems Sciex, #4390812). Three samples each group was iTRAQ-labeled as follows: V1, V2, V3 and C1, C2, C3 were individually labeled with iTRAQ reagent (including V1-iTRAQ 113, V2-iTRAQ 114, V3-iTRAQ 115, C1-iTRAQ 116, C2-iTRAQ 117, C3-iTRAQ 118). Then all the labeled samples were mixed and vacuum dried.

Separation of peptides and LC-MS/MS analysis

These processes were conducted according to routine protocols [13-15]. A RIGOL L-3000 dual gradient HPLC (Puyuanjingdian science and technology Ltd, Beijing, China) coupled with Thermo Scientic EASY-nLC 1000 System (Nano HPLC) were used for analysis. The labeled samples were mixed and dissolved in 100μl of mobile phase A (98% of ddH_2O, 2% of acetonitrile (pH 10), 14,000g, 20min, RT) and the supernatant was collected. High pH reversed-phase chromatography was performed to separate the

trypsin digested peptide. 100μl of sample was loaded onto Durashell-C18 (4. 6 mm×250 mm, 5μm, 100 Å, Agela, DC952505-0) and subjected to a flow rate of 0.7 ml/min of mobile phase B [98% acetonitrile, 2% ddH_2O (pH 10)]. The separation gradient was as follows: 0 min, 5% mobile phase B; 5 min, 8% mobile phase B; 35 min, 18% mobile phase B; 62 min, 32% mobile phase B; 64 min, 95% mobile phase B; 68 min, 95% mobile phase B; 72 min, 5% mobile phase B.

Then the acquired sample was re-suspended with 20μl of 2% carbinol, 0.1% formic acid (12,000r, 10min, RT), and 10μl of supernatant was loaded onto EASY-Spray column (12cm×75μm, C18, 3μm), and a loading pump flow rate was 350 nl/min for 15 min and a separation flow rate was 350 nl/min. The separation gradient was as follows: 0 min, 4% mobile phase B (100% acetonitrile, 0.1% formic acid); 5 min, 15% mobile phase B; 40 min, 25% mobile phase B; 65 min, 35% mobile phase B; 70 min, 95% mobile phase B; 82 min, 95% mobile phase B; 85 min, 4% mobile phase B; 90 min, 4% mobile phase B, as previously described [15-17].

The liquid chromatography eluent was directed into an electrospray ionization source for quantitative time-of-flight MS analysis. Electrospray ionization was performed for information-dependent acquisition in positive-ion mode with a spray voltage of 2.1 kV and a selected mass range of 350-1800 m/z. The Thermo Q-Exactive system was operated in data-dependent acquisition mode, as previously described [13, 18].

Mass spectrometry data processing and protein quantification

In our study, the functional annotations of the differentially expressed proteins were acquired by utilizing the Uniport and Rattus norvegicus database. The mass spectrometry analysis of iTRAQ was carried out by Thermo Q-Exactive mass spectrometry. The original mass spectrometry file was processed by proteome discoverer 1.4 (thermo corporation). The analysis and search parameters were as follows: trypsin as the digestion enzyme with allowance for a maximum of two missed cleavage; Carbamidomethyl (C) as a fixed modification; Oxidation (M), N-terminal, K and iTRAQ 8 plex modification as a dynamic modification; precursor ion mass tolerance of 15ppm; and fragment ion mass tolerance of 20mmu. The division values of differentially expressed proteins were set as follows: a significant difference was considered when the p-value was less than 0.05 and the differentially expressed proteins cutoff value was more than 1.2-fold [14, 19].

Bioinformatics analysis

The differentially expressed proteins were analyzed by GO analysis, the cellular components (CC), the molecular function (MF) and the biological process (BP) involved in the differential protein were analyzed, and the metabolic pathway enrichment analysis was carried out using the KEGG database. A p-value $\leq$ 0.05 was used as the threshold of significant enrichment of GO and KEGG pathways.

Western blot to confirm potential proteins

Western blot was conducted according to routine protocols [6, 7]. The proteins were extracted from the left testicle tissue of rats. 100 ug of protein was subjected to 8% and 12% sodium dodecyl sulfate-polyacrylamide gel electrophoresis and transferred onto polyvinylidene fluoride membranes (EMD Millipore Corporation, Billerica, MA, USA). Membranes were blocked in tris-buffered saline containing 0.1% Tween 20 and 5% nonfat milk powder (TBST) for 3-4 hours at room temperature, then was incubated with the primary antibody overnight at 4 ℃. Antibodies used were as follows: anti-ATP7a (1:1000; ab131400; Abcam, Cambridge, UK), anti-CIB1 (1:500; ZP2168BP68; Boster Biotechnology Co., Wuhan, China), and anti-β-actin (1:5000; I102; Bioworld Technology, Co. Ltd. USA). Four washes with TBST for 10 minutes each followed. The membranes were then incubated with HRP-conjugated secondary antibody (1:5000; BA1054; Boster Biotechnology Co., Wuhan, China) for 1 hour at room temperature. After washing, the specific proteins were visualized by enhanced chemiluminescence and imaged by Chemi DOC XRS$^+$ (Bio-Rad Laboratories, Inc., Hercules, CA, USA). The relative intensity and density of immunoreactive bands was measured using Image J software (National Institute of Health, MD, USA). The results were obtained using at least three separate samples. The relative expression of goal protein was normalized with β-actin as a control.

Statistical analysis

All the statistical analysis and graph preparation were performed using IBM SPSS Statistics version 21.0 (SPSS Inc., Chicago, IL, USA) or GraphPad Prism 6 software (GraphPad Software, Inc., La Jolla, CA, USA). All data were presented as the mean ± standard deviation. The differences between the two groups were compared by independent sample T test. $P<0.05$ was considered to indicate a statistically significant difference.

Results

Changes in histologic structure of rats testis

The layers in the seminiferous tubules of normal group were well organized from external to internal as basal lamina, spermatogonia, spermatocyte, and spermatid. However, the seminiferous epithelium was disorganized and germ cells were seriously reduced in the varicocele group (Fig. 1).

Expression analysis of the candidate protein

In this study, the expression of differential proteins in testicular tissue with varicocele rats were detected by iTRAQ combined with LC-MS/MS. The protein database was searched by protein pilot 4.0 software. In total, 5277 proteins were detected by proteome analysis. Proteins with a relative expression of > 1. 2 or <1.2 and results were regarded as statistically significant at p-values less than 0.05. A total of 65 differentially expressed proteins were identified in the mixed samples of the two groups, of which 31 were up-regulated (Table 1) and 34 were down-regulated (Table 2) (Fig. 2).

GO and KEGG database analysis

GO analysis was conducted to understand the functional basis of the differentially expressed proteins, which were identified by iTRAQ. The biological process (BP), cell component (CC) and molecular function (MF) data were the basic information of GO analysis. The metabolic pathway enrichment of differential proteins were analyzed by R language software. GO analysis showed that the identified proteins were widely distributed in cells, functionally diverse, and involved in a variety of biological processes. CC analysis showed that the identified proteins were mainly distributed in the cytoplasm, nucleus, extracellular region, cytoskeleton, cell membrane, plasma membrane, and mitochondria (Fig. 3a). MF analysis showed that the identified proteins were mainly had the following functions: transporter activity, signal transduction activity, metal ion binding, protein binding, receptor binding and so on (Fig. 3b). BP analysis showed that the identified proteins were mainly involved in signal transduction, protein cycle, transmembrane transport, protein transport, vesicular mediated transport, cell division, membrane tissue, and other biological processes (Fig. 3c). KEGG pathway analysis was conducted to enrich the potential pathways of the identified proteins with differential expression. KEGG analysis showed that the main metabolic pathways involved in the identified proteins were antibiotic biosynthesis and protein processing in endoplasmic reticulum (Fig. 3d).

Western-blot validation

The expression levels of ATP7A and CIB1 in the two groups were detected by western-blot. The result showed that the expression levels of ATP7A and CIB1 in the varicocele group were significantly decreased compared with that in the normal group ($p<0.05$), which was the same as the results of proteome analysis (Fig. 4).

Discussion

Varicocele is a common disease in the male genitourinary system, it is one of the most important causes of male infertility [20]. However, the exact molecular mechanism of varicocele inducing male infertility has not yet been clarified. In this study, the proteome method of iTRAQ combined with LC-MS/MS was used to screen out the new biomarkers that might play an important role in male infertility caused by varicocele. The function of differential proteins was classified by GO analysis, it was found that the main biological functions were binding, signal transduction, protein cycle, transmembrane transport, protein transport and cell division. KEGG results showed that differential proteins were mainly involved in antibiotic biosynthesis and protein processing in endoplasmic reticulum. Among the many screened differential protein molecules, molecules with a more significant difference in protein expression between the two groups, and the functional molecules related to spermatogenesis were reported in the literature as our candidate molecules for further study. ATP7A and CIB1 molecules were selected as candidate molecules. Our study found that the expression of ATP7A and CIB1 in testis of VC rats were significantly lower than that of normal rats in the protein level ($p<0.05$), which is consistent with what proteomic analysis results.

CIB1 was an important calcium-binding regulatory protein of 22 kDa [21]. The expression level of CIB1 was highest in normal testicular tissue, and participated in calcium signaling, cell survival and

proliferation, cell migration, cell adhesion and apoptosis [22, 23]. CIB1 could regulate the release of intracellular Ca^{2+}, the calcium ion signal had special significance in the sperm cells, and it was the central regulator factor of many key activities, which included capacitation, superactivation, chemotaxis and acrosome reaction [24, 25]. The damage of calcium ion signal in sperm was related to male sterility [26]. CIB1 was necessary for spermatogenesis in mice, the deletion of CIB1 may lead to differentiation and dysfunction of Sertoli cells. Sun et al. found that the expression level of CIB1 in patients with oligospermia and asthenospermia were lower than those in the control group, while the cyclin-dependent kinase 1 (CDK1) were significantly increased, and there was a significant correlation between CIB1 mRNA level and CDK1 mRNA level. Therefore, they came to conclusion that CIB1 may be involved in the pathogenesis of oligozoospermia through CDK1 signaling pathway [27]. Yuan et al. found that both mRNA and protein expression levels of Cdc2/Cdk1, a regulatory factor of cell cycle, were significantly higher in mouse testes with CIB1 deletion than that in the control group, and the proliferation rate of the embryonic fibroblasts was significantly reduced, it is suggested that the expression changes of CDK1 and Cdc2 may destroy the normal interval of Sertoli cell proliferation and lead to the imbalance between the number of Sertoli cells and germ cells, which may lead to the increase of germ cell apoptosis and spermatogenesis defects [21, 28]. Therefore, we believe that the decreased expression of CIB1 can be used as an auxiliary biomarker for the diagnosis of varicocele sterility. However, how the decrease of CIB1 leads to male sterility needs further study.

Copper was an essential trace element for normal growth and development of all organisms [29]. It is reported that normal sperm count and sperm motility need to be maintained by physiological copper concentration in seminal plasma, and it was important for spermatogenesis [30, 31]. Kowal et al. found that the copper metabolism disorders could affect the sperm motility, sperm count, sperm head morphology, integrity of plasma membrane in tail cells, and the structure of testicular tissue [32]. In human and animal experiments, male gonads were particularly sensitive to the increase of copper concentration, which leads to the decrease of testosterone level, the degradation of spermatogenic tubule epithelium, the decrease of sperm count and motility, the inhibition of acrosome reaction and spermatogenesis , and the increase of cell apoptosis, so that the fertility of the male was reduced [29-35]. ATP7A could protect tissue from excessive copper and played a crucial role in cellular copper homeostasis [36, 37]. The results of Ogórek et al. showed that the expression of ATP7A could protect the germ cells from the negative effects of excessive copper, and that ATP7A was mainly active in primary spermatocytes [33]. It is suggested that the concentration of copper in vivo should be strictly regulated. Therefore, we speculate that the downregulation of ATP7A expression in testicular tissue of varicocele infertile rats may result in the copper metabolism disorders, which leads to the decrease of sperm count and sperm motility, the increase of apoptosis, and the decrease of male fertility.

Conclusions

In summary, we speculate that ATP7A and CIB1 may be play an important role in normal spermatogenesis and are essential to maintain normal fertility in rat testicular tissue. they may be very important molecules involving in spermatogenesis of varicocele. The decrease of their expressions will probably cause

increased spermatogenic cell apoptosis, further induce increased spermatogenic failure, and finally lead to male infertility.

Abbreviations

VC: varicocele; iTRAQ: isobaric tags for relative and absolute quantitation; LC-MS/MS: liquid chromatography-tandem mass spectrometry; ATP7A: ATPase and Cu^{+} -transporting alpha; CIB1: calcium and integrin-binding protein 1; GO: gene ontology; KEGG: kyoto encyclopedia of genes and genomes; RT: room temperature; CC: cellular components; MF: molecular function; BP: biological process; TBST: tris-buffered saline containing 0.1% Tween 20 and 5% nonfat milk powder; CDK1: cyclin-dependent kinase 1.

Declarations

Acknowledgements

Not applicable.

Author Contributions

Q.Q.,concept and design, analysis, acquisition proteomics data, interpretation of data, drafting of the article, revision of the article, and final approval for submission. X.F.L., W.Z., interpretation of data, drafting of the article, revision of the article, and final approval for submission. Y.M.W., F.Z., and J.R.L. participated in the interpretation of data, revision of the article, and final approval for submission. D.F.W., C.X.Y., discussion of results, drafting of the article, and final approval for submission. All authors have read and approved the final version and submission of this manuscript.

Funding

Supported by the National Natural Science Foundation of China (81401192 and 81973864), Research Project Supported by Shanxi Scholarship Council of China (2017123) and Fund Program for the Scientific Activities of Selected Returned Overseas Professionals in Shanxi Province.

Availability of data and materials

All data are stored in the form of an electronic database together and results from analysis in the form of a statistical software report.

Ethics approval and consent to participate

All authors declare that this research was done by strictly adhering to the rules of good scientific practice and are responsible for its content. All experiments were performed in a manner that maximized rigor and reproducibility and without bias. All applicable international, national and/or institutional guidelines for the care and use of animals were followed. All animal experiments conformed with the Guide for Care and Use of Laboratory Animals and were approved by Shanxi Provincial People's Hospital.

Consent for publication

All authors consent to the publication of this manuscript.

Competing interests

The authors declare that they have no conflict of interest.

Author details

[1] Pediatrics Department, Shanxi Provincial People's Hospital Affiliated to Shanxi Medical University,

Shanxi, China; [2] Biochemistry and Molecular Biology, Basic Medical College, Shanxi Medical University, Shanxi, China; [3] Reproductive Medical Department, Shanxi Provincial People's Hospital Affiliated to Shanxi Medical University, Shanxi, China; [4] Central Laboratory, Shanxi Provincial People's Hospital Affiliated to Shanxi Medical University, Shanxi, China;

References

1. Sheehan MM, Ramasamy R, Lamb DJ. Molecular mechanisms involved in varicocele-associated infertility. J Assist Reprod Genet.2014; 31: 521-6.
2. Clavijo RI, Carrasquillo R, Ramasamy R. Varicoceles: prevalence and pathogenesis in adult men. Fertil Steril.2017; 108: 364-9.
3. Alsaikhan B, Alrabeeah K, Delouya G, Zini A. Epidemiology of varicocele. Asian J Androl.2016; 18:179-81.
4. Razi M, Malekinejad H. Varicocele-induced infertility in animal models. Int J Fertil Steril.2015; 9:141-9.
5. Cho CL, Esteves SC, Agarwal A. Novel insights into the pathophysiology of varicocele and its association with reactive oxygen species and sperm DNA fragmentation. Asian J Androl.2016; 18: 186-9.
6. Qin Q, Liu J, Ma Y, Wang Y, Zhang F, Gao S, et al. Aberrant expressions of stem cell factor/c-KIT in rat testis with varicocele. J Formos Med Assoc.2017; 116: 542-8.
7. Zhao W, Liu JR, Wang DF, Wang YM, Zhang F, Jin GR, et al. Effect of silencing HIF-1α gene on testicle spermatogenesis function in varicocele rats. Cell Tissue Res.2019; 378: 543-54.
8. Liang M, Wen J, Dong Q, Zhao LG, Shi BK. Testicular hypofunction caused by activating p53 expression induced by reactive oxygen species in varicocele rats. Andrologia.2015; 10: 1175-82.
9. Ghandehari-Alavijeh R, Tavalaee M, Zohrabi D, Foroozan-Broojeni S, Abbasi H, Nasr-Esfahani MH. Hypoxia pathway has more impact than inflammation pathway on etiology of infertile men with varicocele. Andrologia. 2019; 51: e13189.
10. Hou S, Xian L, Shi P, Li C, Lin Z, Gao X. The magea gene cluster regulates male germ cell apoptosis without affecting the fertility in mice. Sci Rep.2016; 6: 26735.

11. Turner TT. The study of varicocele through the use of animal models. Hum Reprod Update.2001; 7:78-84.
12. Yao B, Zhou WL, Han DY, Ouyang B, Chen X, Chen SF, et al. The effect of the degree of left renal vein constriction on the development of adolescent varicocele in Sprague-Dawley rats. Asian J Androl.2016; **18:** 471-4.
13. Shen L, Liao L, Chen C, Guo Y, Song D, Wang Y, et al. Proteomics Analysis of Blood Serums from Alzheimer's Disease Patients Using iTRAQ Labeling Technology. J Alzheimers Dis.2017; 56: 361-78.
14. Pang XM, Zhou X, Su SY, Chen CY, Wei ZX, Tao YF, et al. Identification of Serum Biomarkers for Ischemic Penumbra by iTRAQ-Based Quantitative Proteomics Analysis. Proteomics Clin Appl. 2019; 13: e1900009.
15. Wang Y, Zhang X, Huang G, Feng F, Liu X, Guo R, et al. iTRAQ-Based Quantitative Analysis of Responsive Proteins Under PEG-Induced Drought Stress in Wheat Leaves. Int J Mol Sci.2019; 20: 2621.
16. Hua YJ, Wang SN, Zou LS, Liu XH, Xu JY, Hou Y, et al. iTRAQ-based quantitative proteomics of cultivated Pseudostellaria heterophylla and its wild type. Yao Xue Xue Bao.2016; 51: 475-85.
17. Liu CW, Zhang Q. Isobaric Labeling-Based LC-MS/MS Strategy for Comprehensive Profiling of Human Pancreatic Tissue Proteome. Methods Mol Biol.2018; 1788: 215-24.
18. Chu C, Yan N, Du Y, Liu X, Chu M, Shi J, et al. iTRAQ-based proteomic analysis reveals the accumulation of bioactive compounds in Chinese wild rice (Zizania latifolia) during germination. Food Chem.2019; 15: 635-44.
19. Xu F, Gao QQ, Zhu LL, Jiang HS, Chen H, Xu ZP, et al. Impact of varicocelectomy on the proteome profile of testicular tissues of rats with varicocele. Andrologia.2018; 50:12873.
20. Chiba K, Ramasamy R, Lamb DJ, Lipshultz LI. The varicocele: diagnostic dilemmas, therapeutic challenges and future perspectives. Asian J Andro.2016; 18: 276-81.
21. Yuan W, Leisner TM, McFadden AW, Clark S, Hiller S, Maeda N, et al. CIB1 is essential for mouse spermatogenesis. Mol Cell Biol.2006; 26; 8507-14.
22. Leisner TM, Freeman TC, Black JL, Parise LV. CIB1: a small protein with big ambitions. FASEB J .2016; 30: 2640-50.
23. Yu Y, Song X, Du L, Wang C. Molecular characterization of the sheep CIB1 gene. Mol Biol Rep.2009; 36: 1799-809.
24. Rahman MS, Kwon WS, Pang MG. Calcium influx and male fertility in the context of the sperm proteome: an update. Biomed Res Int.2014; 841615.
25. Valsa J, Skandhan KP, Khan PS, Avni KP, Amith S, Gondalia M. Calcium and magnesium in male reproductive system and in its secretion. I. Level in normal human semen, seminal plasma and spermatozoa. Urologia.2015; 82:174–8.
26. Beigi Harchegani A, Irandoost A, Mirnamniha M, Rahmani H, Tahmasbpour E, Shahriary A. Possible mechanisms for the effects of calcium deficiency on male infertility. Int J Fertil Steril.2019; 12: 267-72.

27. Sun W, Guan Q, Wen J, Zhang Q, Yang W, Zhang B, et al. Calcium-and integrin-binding protein-1 is down-regulated in the sperm of patients with oligoasthenozoospermia: CIB1 expression in patients with oligoasthenozoospermia. J Assist Reprod Genet.2014; 31: 541-7.
28. Urano A, Endoh M, Wada T, Morikawa Y, Itoh M, Kataoka Y, et al. Infertility with defective spermiogenesis in mice lacking AF5q31, the target of chromosomal translocation in human infant leukemia. Mol Cell Biol. 2005; 25: 6834-45.
29. Kardos J, Héja L, Simon Á, Jablonkai I, Kovács R, Jemnitz K. Copper signalling: causes and consequences. Cell Commun Signal.2018; 16: 71.
30. Bolanca I, Obhodas J, Ljiljak D, Matjacic L, Kuna K. Synergetic effects of K, Ca, Cu and Zn in human semen in relation to parameters indicative of spontaneous hyperactivation of spermatozoa. PLoS One.2016; 11: e0152445.
31. Suarez SS. Control of hyperactivation in sperm. Hum Reprod Update.2008; 14: 647-57.
32. Kowal M, Lenartowicz M, Pecio A, Gołas A, Błaszkiewicz T, Styrna J. Copper metabolism disorders affect testes structure and gamete quality in male mice. Syst Biol Reprod Med.2010; 56: 431-44.
33. Ogórek M, Lenartowicz M, Starzyński R, Jończy A, Staroń R, Doniec A, et al. Atp7a and Atp7b regulate copper homeostasis in developing male germ cells in mice. Metallomics.2017; 9: 1288-303.
34. Liu JY, Yang X, Sun XD, Zhuang CC, Xu FB, Li YF. Suppressive effects of copper sulfate accumulation on the spermatogenesis of rats. Biol Trace Elem Res.2016; 174: 356-61.
35. Sakhaee E, Emadi L, Abshenas J, Kheirandish R, Azari O, Amiri E. Evaluation of epididymal sperm quality following experimentally induced copper poisoning in male rats. Andrologia.2012; 44: 110–6.
36. Ogórek M, Herman S, Pierzchała O, Bednarz A, Rajfur Z, Baster Z, et al. Molecular machinery providing copper bioavailability for spermatozoa along the epididymial tubule in mouse. Biol 7
37. Lutsenko S, Barnes NL, Bartee MY, Dmitriev OY. Function and regulation of human copper-transporting ATPases. Physiol Rev.2007; 87: 1011–46.

Tables

Table 1 List of significantly up-regulated proteins between normal and varicocele tissues which was identified using iTRAQ coupled with LC-MS/MS ($P<0.05$).

Accession	Gene Name	Log Ratio (2/1)	P Value
A0A0G2JSH5	Alb	0.362092919	0.00013281
A0A0G2JST3	Krt1	0.42075115	0.000720546
A0A0G2JUU5	Krt83	1.816228873	0.00031862
A0A0G2JWP1	Cstf2	0.28473846	0.00665261
A0A0G2JWX4	Krt2	0.367011662	0.031284948
A0A0G2JXU4	Cyp2a3	0.54711915	0.024805978
A0A0G2JXX5	LOC103694487	0.917790203	0.015879463
A0A0G2K0R4	Maz	0.338547209	0.022041612
A0A0G2K477	Ighm	0.35223196	0.00379313
A0A0H2UHM4	Odf2	0.52928052	0.027655982
P11711	Cyp2a1	0.493689001	0.000573233
D3ZAK6	Rps15-ps2	1.889894445	0.031240492
D3ZEA3	Grb10	0.373034925	0.005821532
D4A4W6	Slirp	0.264467072	0.029918106
F1LSK5	Heatr5a	0.360844625	0.02564106
F1LUB9	Ccdc38	0.769446258	0.007932682
G3V7N5	Cpt2	1.29731554	1.87521E-06
P00502	Gsta1	0.400297192	0.003801095
P20761	Igh-1a	0.429823557	0.002582838
P20762		0.482181168	0.003137436
Q6IFU8	Krt17	1.27473808	0.000131779
Q6IFU7	Krt42	0.844989371	8.92335E-05
Q6P6Q2	Krt5	0.721714816	0.000227475
Q4FZU2	Krt6a	0.517642375	0.005250149
Q6IG05	Krt75	0.940405875	0.000137205
M0R7B4	Hist1h1d	0.778775753	0.006506709
M0RAV0		0.276758124	0.013250635
Q6AYU1	Morf4l1	0.269547274	0.015341756
Q9ET64	Smpd2	0.956027847	0.043944135
Q6IFU9	Krt16	0.794802723	0.000746155
P05545	Serpina3k	0.676052872	1.08437E-05

Table 2 List of significantly down-regulated proteins between normal and varicocele tissues which was identified using iTRAQ coupled with LC-MS/MS ($P<0.05$).

Accession	Gene Name	Log Ratio (2/1)	P Value
P22072	Hsd3b	-0.349942471	0.010382497
A0A0G2JSK1	Serpina3c	-0.988783656	8.21981E-05
A0A0G2JUA0	Desi2	-0.363279195	0.001599056
A0A0G2JUH7	Spag8	-0.406432931	0.044488653
A0A0G2JVW3	Ankrd17	-0.269485939	0.038925282
A0A0G2K6V9	RGD1565071	-0.373390951	0.043321306
A0A0G2K8V1	Atp11a	-0.527381912	0.037056552
P02770	Alb	-0.338314643	0.000185889
P70705	Atp7a	-0.478523512	0.047977857
Q8CJB9	Rnf40	-0.37442439	0.013003884
P47728	Calb2	-0.36972081	0.007936968
Q9EQV8	Cpn1	-0.394315952	0.034775994
Q9R010	Cib1	-0.44018114	0.01179658
P18886	Cpt2	-0.304036252	0.029037976
D3Z9C2	Fam50b	-0.440113873	0.037562144
D3ZDJ9	Bicc1	-0.928955624	0.030850589
D3ZH41	Ckap4	-0.343508377	0.024139485
D3ZMR9	Mrpl21	-0.337430409	0.013521404
D4A6L3	Nol8	-0.300726201	0.014066054
F1LSD3	Itgb4	-0.589493452	0.016118851
F1LWZ8	Lemd3	-0.334686286	0.039224606
F1M276	Fam81b	-0.357674916	0.005276258
F1M4N6	Dock3	-0.273520913	0.014734841
F1M5Q6	Fbxo21	-0.507965101	0.028385471
Q9WUS0	Ak4	-0.272692859	0.040115309
Q3KR73	Kansl3	-0.286149786	0.049094498
M0R5K4	Gm21812	-0.644121285	0.003529323
Q6VEU1	Nob1	-0.350190323	0.014499704
P22057	Ptgds	-0.285524373	0.014267
Q4V794	Vps37a	-0.280429894	0.019530985
Q5XIQ6	Trmt2a	-0.285631296	0.036267533
P24051	Rps27l	-0.317633443	0.018055559
Q6AYP6	Saxo1	-0.323878446	0.020279433
Q91ZW6	Tmlhe	-0.272860354	0.017575565

Figures

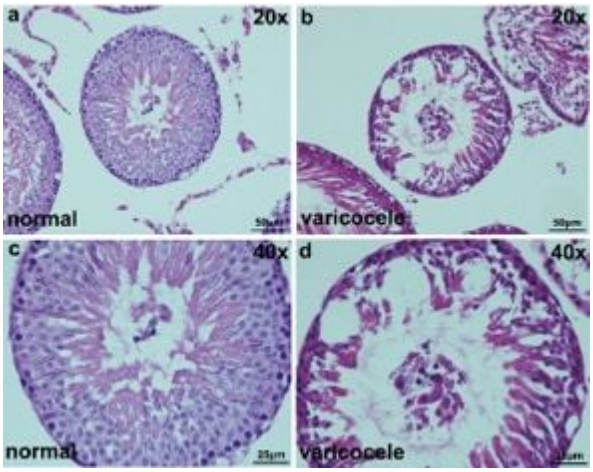

Figure 1

Upper panel shows the morphology of seminiferous tubules. Testis tissues in the normal group (a, c) and varicocele group (b, d) were analyzed using hematoxylin and eosin stain (magnification, × 200, ×400).

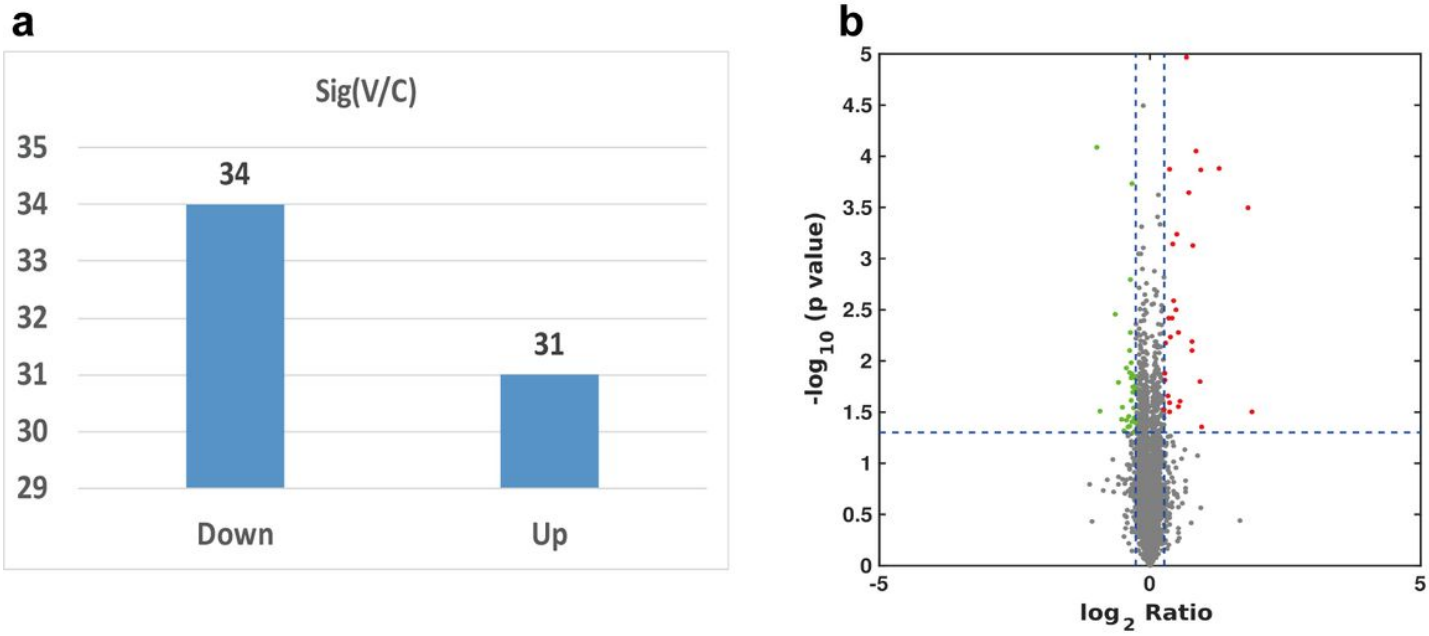

Figure 2

(a) The results of histogram of differentially expressed proteins showed that there were 34 down-regulated proteins and 31 up-regulated protein. (b) Ratio distribution of all quantitative proteins. Differentially expressed protein marked in red or green (red indicates upregulation and green indicates downregulation).

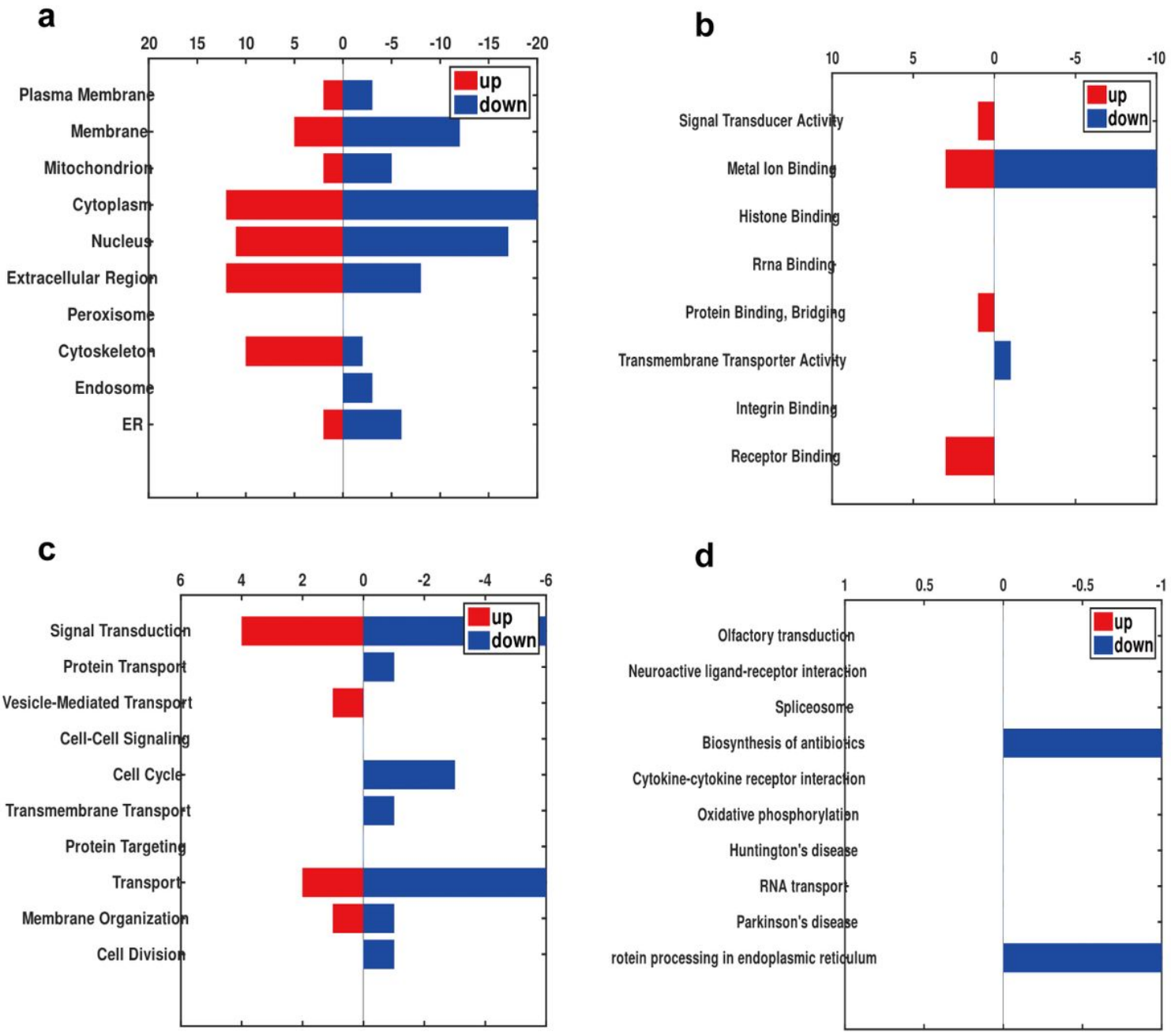

Figure 3

Top 10 enrichment in GO analysis of the differentially expressed proteins. All identified proteins were functionally annotated in GO database according to their cellular component (a), molecular function (b), and biological process (c). (d) Top 10 enrichment in KEGG pathway maps of the differentially expressed proteins.

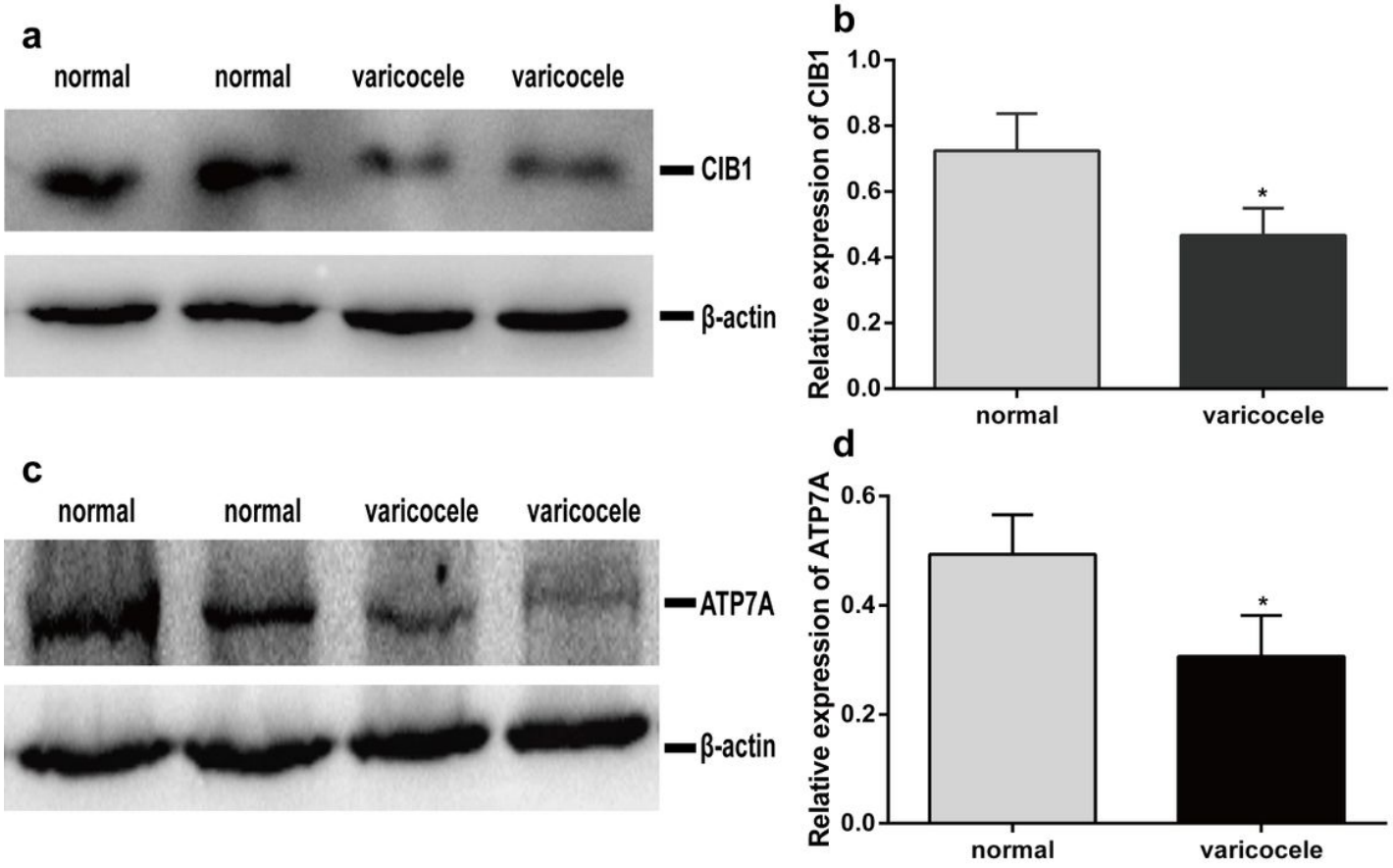

Figure 4

Validation of differentially expressed proteins by western blot analysis. β-actin was used as loading control. (a) Western blot analyses of CIB1 in the varicocele group and normal group, β-actin was used as loading control. The gels were run under the same experimental conditions. (b) The expression of CIB1 were semi quantified by densitometry. (c) Western blot analyses of ATP7A in the varicocele group and normal group, β-actin was used as loading control. The gels were run under the same experimental conditions. (d) The expression of ATP7A were semi quantified by densitometry. *P<0.05 versus normal group.